© 2017. Published by The Company of Biologists Ltd | Development (2017) 144, 3264-3277 doi:10.1242/dev.155473

RESEARCH ARTICLE

# Maternal expression of the histone demethylase Kdm4a is crucial for pre-implantation development

**Aditya Sankar[1,2,3,*,§], Susanne Marije Kooistra[1,2,‡,§], Javier Martin Gonzalez[4], Claes Ohlsson[6], Matti Poutanen[5,6] and Kristian Helin[1,2,3,¶]**

## ABSTRACT

Regulation of chromatin composition through post-translational modifications of histones contributes to transcriptional regulation and is essential for many cellular processes, including differentiation and development. KDM4A (JMJD2A) is a lysine demethylase with specificity towards di- and tri-methylated lysine 9 and lysine 36 of histone H3 (H3K9me2/me3 and H3K36me2/me3). Here, we report that *Kdm4a* as a maternal factor plays a key role in embryo survival and is vital for female fertility. *Kdm4a*$^{-/-}$ female mice ovulate normally with comparable fertilization but poor implantation rates, and cannot support healthy transplanted embryos to term. This is due to a role for Kdm4a in uterine function, where its loss causes reduced expression of key genes involved in ion transport, nutrient supply and cytokine signalling, which impact embryo survival. In addition, a significant proportion of Kdm4a-deficient oocytes displays a poor intrinsic ability to develop into blastocysts. These embryos cannot compete with healthy embryos for implantation *in vivo*, highlighting *Kdm4a* as a maternal effect gene. Thus, our study dissects an important dual role for maternal Kdm4a in determining faithful early embryonic development and the implantation process.

**KEY WORDS: Epigenetics, Female fertility, Histone demethylase, Pre-implantation development, Maternal effect, Transcription**

## INTRODUCTION

Epigenetic regulation through DNA methylation and modification of histone proteins is involved in the control and stabilization of gene expression programmes throughout development and proliferation. As such, enzymes responsible for the addition and removal of epigenetic marks on chromatin contribute to a wide variety of biological processes. Many such enzymes have been identified, usually with exquisite specificity for substrate and amino acid residue, as well as type and degree of modification (Greer and Shi, 2012; Kooistra and Helin, 2012; Dimitrova et al., 2015).

Similar to the other members of the JMJD2/KDM4 family of histone demethylases, KDM4A is capable of removing di- and tri-methylation from lysines 9 and 36 of histone H3 (Cloos et al., 2006; Klose et al., 2006; Whetstine et al., 2006; Chen et al., 2006, 2007; Ng et al., 2007). KDM4A, like KDM4C, binds to tri-methylated lysine 4 on histone H3 (H3K4me3) through its double Tudor domain (Huang et al., 2006; Pedersen et al., 2016, 2014). In this way, the KDM4 proteins provide a failsafe mechanism to prevent spurious accumulation of H3K9me3 at active promotors, thereby maintaining transcriptional competence (Pedersen et al., 2016).

KDM4A is overexpressed in several types of cancers (Berry and Janknecht, 2013; Berry et al., 2012; Li et al., 2012, 2011; Shin and Janknecht, 2007; Patani et al., 2011; Slee et al., 2012; Cloos et al., 2006), where it may contribute to cancer cell survival by binding to hormone receptors (Shin and Janknecht, 2007) or by leading to re-replication of specific genomic loci (Black et al., 2013). The other KDM4 family members KDM4B and KDM4C have also been linked to cancer development and maintenance (Kooistra and Helin, 2012; Agger et al., 2016; Cheung et al., 2016), and the proteins are therefore considered as attractive targets for the treatment of cancer patients (Chin and Han, 2015; Hojfeldt et al., 2013).

Injection of *KDM4A* and *Kdm4d* mRNAs have been shown to decrease an H3K9me3 barrier in somatic cell nuclear transfer (SCNT)-mediated reprogramming of human and mouse oocytes, respectively, resulting in dramatic improvement of healthy blastocyst-forming capacity (Chung et al., 2015; Matoba et al., 2014). Similarly, in mouse, Kdm4b was identified as the key factor for two-cell arrest of cloned embryos (Liu et al., 2016). Although these findings present new improved possibilities in reprogramming and fertility research, the physiological role of the KDM4 proteins during normal development have so far not been addressed in detail. Recent studies have shown that individual Kdm4 proteins are dispensable for embryonic development and postnatal life (Kawazu et al., 2011; Pedersen et al., 2014, 2016; Iwamori et al., 2011). Functional redundancy has been described for the Kdm4 family; the combined functions of Kdm4a and Kdm4c are required for embryonic stem cell self-renewal and early embryogenesis (Pedersen et al., 2016).

Here, we have investigated the role of Kdm4a in early mouse development and fertility. We demonstrate that female mice lacking Kdm4a are infertile, and show that the protein is required both as a maternal factor in the oocyte, and in the uterus for proper gene expression during pre-implantation development.

## RESULTS

### *Kdm4a*$^{-/-}$ females are infertile

To investigate the physiological role of *Kdm4a* during normal development, we generated *Kdm4a*$^{-/-}$ knockout mice in a C57Bl/6 background as recently described (Pedersen et al., 2016). Owing to

[1]Biotech Research and Innovation Centre, University of Copenhagen, Copenhagen 2200, Denmark. [2]Centre for Epigenetics, University of Copenhagen, Copenhagen 2200, Denmark. [3]The Danish Stem Cell Center (Danstem), Faculty of Health and Medical Sciences, University of Copenhagen, Copenhagen 2200, Denmark. [4]Core Facility for Transgenic Mice, Faculty of Health and Medical Sciences, University of Copenhagen, 2200 Copenhagen, Denmark. [5]Centre for Bone and Arthritis Research, Institute of Medicine, The Sahlgrenska Academy, University of Gothenburg, Gothenburg 41345, Sweden. [6]Department of Physiology Turku Center for Disease Modeling (TCDM), Institute of Biomedicine, University of Turku, 20520 Turku, Finland.
*Present Address: Centre for Chromosome Stability, Institute of Cellular and Molecular Medicine, University of Copenhagen, 2200 Copenhagen, Denmark.
‡Present Address: Department of Neuroscience, University Medical Centre, Groningen, University of Groningen, 9713 AV Groningen, The Netherlands.
§These authors contributed equally to this work

¶Author for correspondence (kristian.helin@bric.ku.dk)

J.M.G., 0000-0002-7075-6028; K.H., 0000-0003-1975-6097

**Received 28 May 2017; Accepted 14 August 2017**

Development (2017) 144, 3264-3277 doi:10.1242/dev.155473

excision of exon 3, a critical exon that is upstream of the catalytic JmjC domain, the knockout allele can only produce a very short truncated form of Kdm4a (Fig. 1A, Fig. S1A). Thus, a functional Kdm4a protein is not present in the knockout mice (Pedersen et al., 2016).

*Kdm4a*$^{+/-}$ animals were fertile; however, upon inter-crossing heterozygous animals we observed an under-representation of *Kdm4a*$^{-/-}$ mice (16-17% homozygotes in lieu of the expected 25%) at the time of weaning that was not gender specific (Fig. S1B)

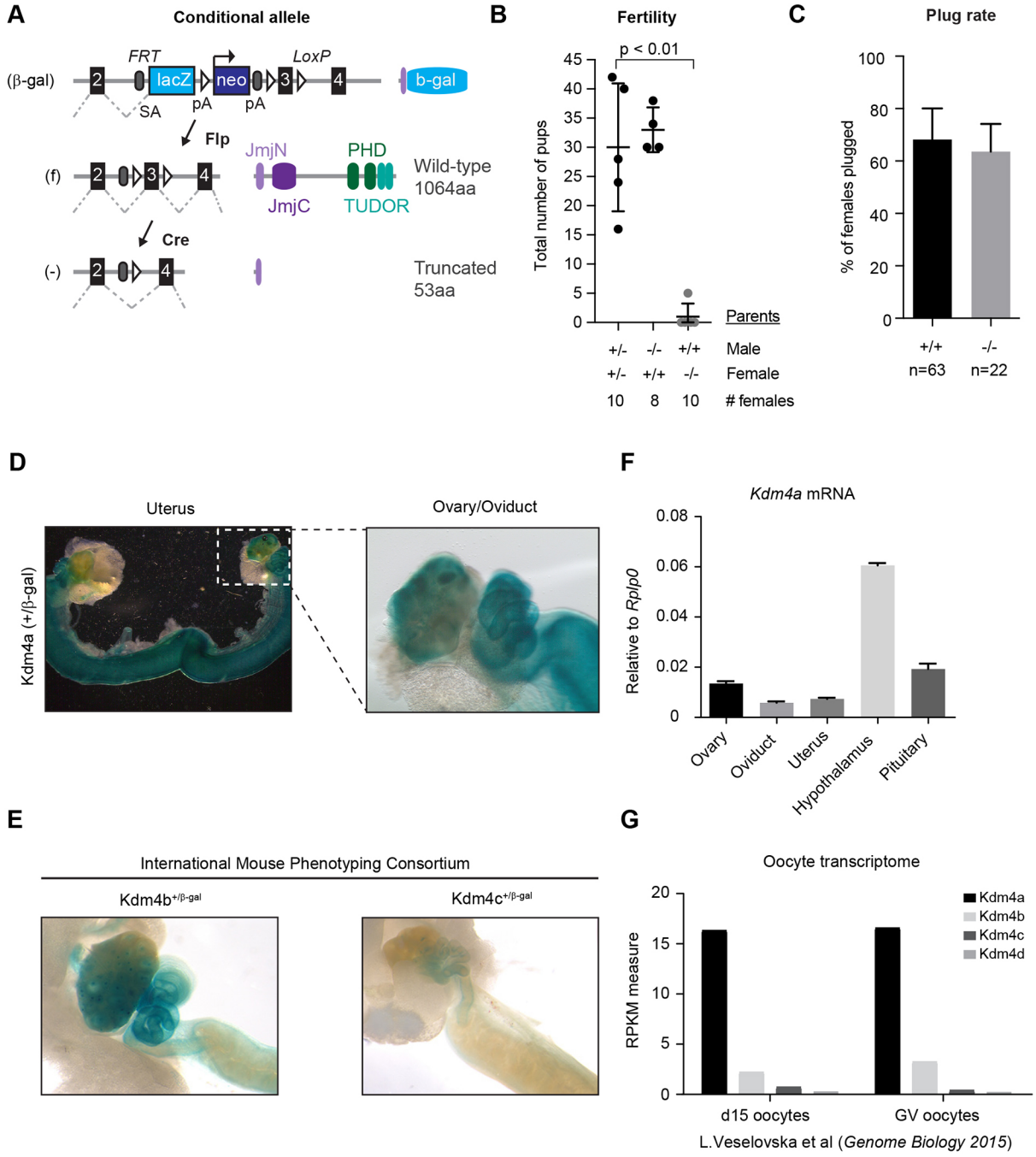


**Fig. 1. *Kdm4a* knockout females are infertile.** (A) Schematics of the *Kdm4a* allele, the targeting cassette, the generation of the *Kdm4a* (–) allele and the resulting wild-type and truncated proteins. (B) Breeding cages with one male and two females of the indicated genotypes were set up and monitored for 4 months. All pups were weaned and removed from the breeding cages at the age of 3 weeks. The total number of pups born per cage ($n$=5, 4 and 5 for cages having *Kdm4a*$^{+/-}$, *Kdm4a*$^{+/+}$ and *Kdm4a*$^{-/-}$ females) is presented with s.d. and significance determined using an unpaired $t$-test. (C) Wild-type ($n$=63) and *Kdm4a*$^{-/-}$ ($n$=22) females were set up for timed mating with wild-type males. The proportion of females that displayed a successful vaginal plug over one week was noted. Data are presented as mean with s.d. and unpaired $t$-test was used to determine statistical significance. (D) β-Galactosidase staining of embryos at the indicated stages expressing the *lacZ* reporter gene under control of the endogenous *Kdm4a* promoter (+/β-gal). Wild-type embryos (+/+) were used as control (not shown). (E) β-Galactosidase staining of female reproductive organs in which the *lacZ* reporter gene is under control of the endogenous *Kdm4b* (EUCOMM) or *Kdm4c* (KOMP) promoter. Images are reproduced with permission from data generated by the respective image-producing centres at EUCOMM and KOMP, which are part of the International Mouse Phenotyping Consortium (IMPC). (F) RT-qPCR for *Kdm4a* in the highlighted tissues ($n$=3) normalized to expression of the housekeeping gene *Rplp0*. Data are presented as mean with s.d. (G) Normalized expression levels in reads per kilobase of transcript per million mapped reads (RPKM) of *Kdm4* family members in murine oocytes (figure created using published data from Veselovska et al., 2015; GEO accession number GSE70116).

Development (2017) 144, 3264-3277 doi:10.1242/dev.155473

(Pedersen et al., 2016). By following the general health of postnatal mice up to 30 weeks of age, we observed no effect of *Kdm4a* deletion on general viability with normal mortality rates in *Kdm4a*$^{-/-}$ animals (Fig. S1C-E). *Kdm4a*$^{-/-}$ males showed slightly reduced weight 8 weeks after birth, but this difference was not sustained (Fig. S1F,G). These results suggest that *Kdm4a*$^{-/-}$ mice are in general viable and develop normally.

To analyse the fertility of *Kdm4a*$^{-/-}$ animals, we set up a breeding test (one male and two females per cage, five cages per group, all pups were weaned and removed from the breeding cages after 3 weeks). During a study period of 4 months, we observed that all null males were fertile and produced litter sizes comparable to heterozygous controls. Of the *Kdm4a*$^{-/-}$ females studied, there was only one female that delivered five pups in three litters during this period (litter sizes of one, two and two). Of the five pups, only two reached weaning age, and the others died within 24 h after birth (Fig. 1B). This indicates that *Kdm4a*$^{-/-}$ females are unable either to mate normally or to sustain pregnancies.

To investigate the lack of fertility in the *Kdm4a*$^{-/-}$ females, we set up timed mating of control and *Kdm4a*$^{-/-}$ females to monitor their mating behaviour. Using littermate controls and wild-type males of proven fertility as breeding partners, we could establish similar numbers of females with vaginal plugs after 5 days (Fig. 1C). In summary, these results show that *Kdm4a* can be deleted from the embryonic genome without consequences for embryonic development and general viability, but it is required postnatally as a maternal determinant of embryonic survival.

### Kdm4a is abundantly expressed in the female reproductive tract

Given that female infertility can be the result of alterations in the mother, the embryo or both, we decided to profile the expression of *Kdm4a* in the reproductive tract. Using the β-galactosidase reporter gene under control of the *Kdm4a* promoter (Fig. 1A), we determined that *Kdm4a* is expressed in several tissues throughout embryonic development (Fig. S1H). In the adult female reproductive tract, *Kdm4a* is highly expressed in the ovary, oviduct and uterus (Fig. 1D). In comparison, although *Kdm4b* is expressed at a low level in the ovary (Fig. 1E) (Brown and Moore, 2012), both male and female *Kdm4b* null mice are fully fertile (K. Agger and K.H., unpublished results). *Kdm4c*, the functionally redundant homologue of *Kdm4a* (Pedersen et al., 2016), shows little to no expression (Fig. 1E) in the female reproductive system (Brown and Moore, 2012). Additionally, *Kdm4c* transcripts are absent in murine oocytes, and only begin to appear later in cleavage embryos during embryonic genome activation (Dahl et al., 2016), suggesting that embryos cannot intrinsically compensate for the loss of *Kdm4a* during this period.

Gene expression analysis showed that *Kdm4a* is expressed in all tissues relevant to the female reproductive system – namely, hypothalamus, pituitary, ovary, oviduct and uterus (Fig. 1F). Immunohistochemical studies on the ovary revealed a strong and specific expression of *Kdm4a* in oocytes and surrounding developing follicles (Fig. S1I). In agreement with this, a murine oocyte transcriptome study showed expression of *Kdm4a* in developing and mature oocytes (Veselovska et al., 2015). At these stages of oocyte development, there is relatively abundant expression of *Kdm4a*, but not of *Kdm4b/c/d* transcripts (Fig. 1G), suggesting that Kdm4a could impact on embryo survival directly through its presence in the oocyte. Taken together, these results show that *Kdm4a* is expressed throughout the female reproductive axis and that, of the Kdm4 family, only Kdm4a is expressed in the oocyte.

### *Kdm4a*$^{-/-}$ females have low embryo implantation rates with poor developmental potential

Because we observed successful mating behaviour, we wanted to understand whether the infertility was a function of poor gametogenesis or maternal tract defects resulting in loss of pregnancy. We observed no gross morphological alterations in *Kdm4a*$^{-/-}$ uterus, ovaries and oviduct (Fig. S2). Closer immunohistological inspection revealed reproductive organ structures with normal proliferative capacity and absence of any excessive cell death through apoptosis (Fig. S3A,B, Table S1).

Next, we tested ovulation capacity using hormone-induced superovulation of immature females (4-5 weeks old). We established that *Kdm4a*$^{-/-}$ females produced similar numbers of oocytes compared with littermate controls (Fig. 2A), suggesting normal gametogenesis. By using timed mating of young adult females, we screened for the presence of embryos at mid-gestation [9.5 days post-coitum (dpc)] and found that 75% of successfully plugged *Kdm4a*$^{-/-}$ females did not show any evidence of embryos or decidualization (Fig. 2B). This result suggests a developmental failure in embryos of *Kdm4a*$^{-/-}$ females prior to implantation. Next, we assessed the decidua within the 25% of females that showed evidence of implantation. These females contained a comparable number of implantation sites to controls; however, upon inspecting the decidua in these females, we observed that 80% contained embryos that were developmentally delayed or resorbed (Fig. 2C,D).

Because our results demonstrate that embryos do not implant efficiently in *Kdm4a*$^{-/-}$ females, we assessed the state of pre-implantation embryos. To do this, we performed natural timed mating of mature virgin (7-8 weeks old) *Kdm4a*$^{-/-}$ females and littermate controls. Following successful mating, the embryos were flushed from the oviduct at 2.5 dpc to study their developmental state. Strikingly, we found that the majority of embryos from *Kdm4a*$^{-/-}$ females were developmentally delayed or arrested already at 2.5 dpc with very few having developed beyond the 2- to 4-cell stage (Fig. 2E,F). This is despite the production of a similar number of embryos per female in both groups (Fig. 2F), which is consistent with our ovulation data (Fig. 2A).

Similarly, embryos isolated at 3.5 dpc that were subsequently cultured overnight displayed a poor ability to cavitate, a pre-requisite for successful implantation (Fig. S4A). Only 20% of maternal mutant *Kdm4a* embryos hatched to establish embryonic stem cell lines when transferred to naïve pluripotent mouse embryonic stem cell (mESC) growth (2i+LIF) conditions (Fig. S4B). These results establish that *Kdm4a*$^{-/-}$ females ovulate and fertilize embryos normally but have low implantation rates with the majority of embryos being defective during pre-implantation development.

### Kdm4a is required in the maternal reproductive tract to establish pregnancy

Given that *Kdm4a* is abundantly expressed in all reproductive tissues, particularly in the uterus, where expression of its redundant homologue *Kdm4c* is largely absent, we used embryo transplantation to understand whether Kdm4a is required in an embryo-extrinsic manner to establish pregnancy. Simultaneously, we transferred wild-type two-cell embryos into wild-type and *Kdm4a*$^{-/-}$ pseudo-pregnant recipients. Six out of nine wild-type recipient mice delivered healthy pups with litter sizes ranging from four to six pups per female. However, none of the eight *Kdm4a*$^{-/-}$ recipient females delivered any pups (Fig. 3A). Importantly, the *Kdm4a*$^{-/-}$ recipient mothers did not show any evidence of embryo implantation.

Development (2017) 144, 3264-3277 doi:10.1242/dev.155473

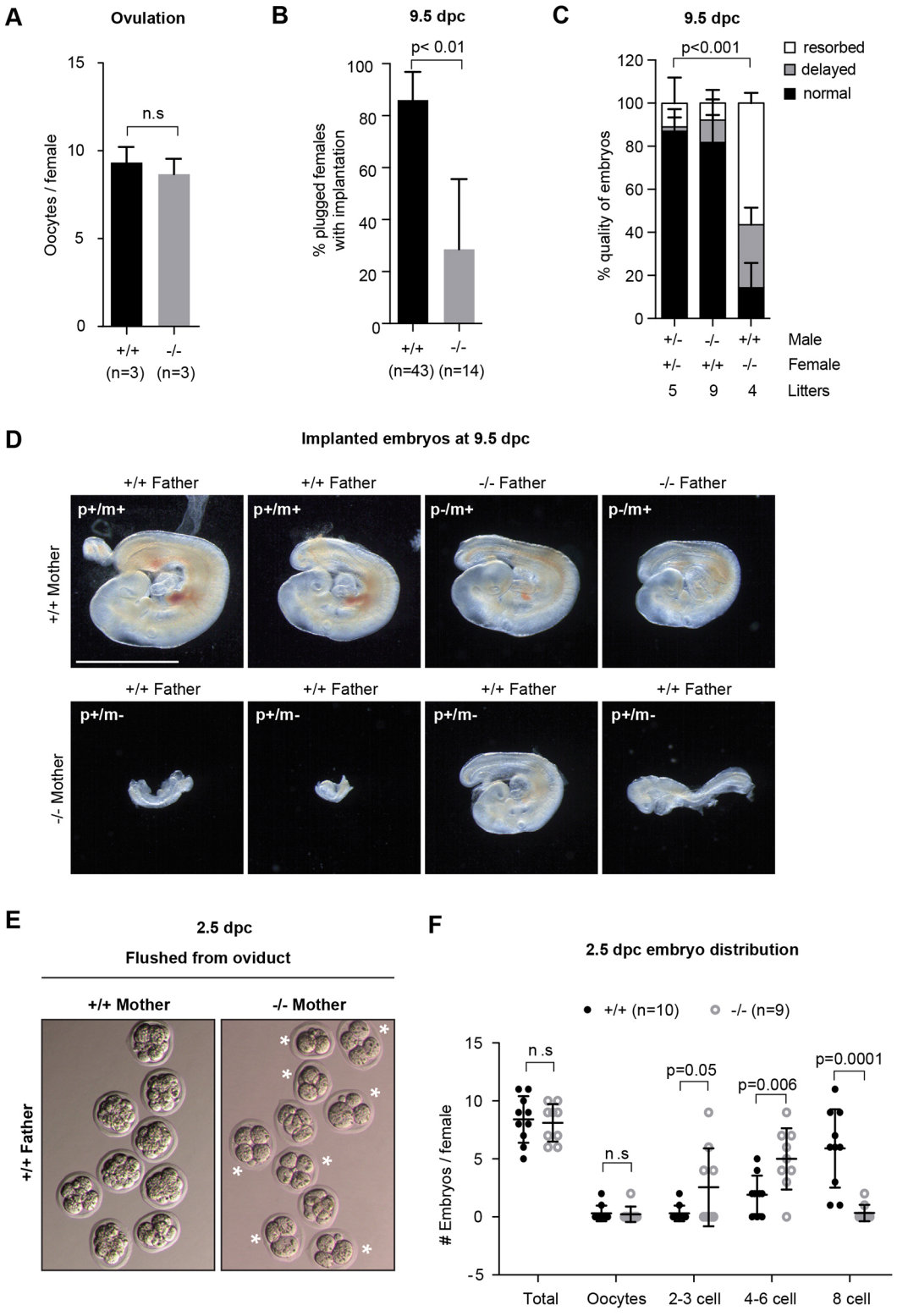


**Fig. 2.** See next page for legend.

We hypothesized that *Kdm4a*$^{-/-}$ females do not support early pregnancy, because of hormonal defects or defective gene expression related to implantation in the uterus. Reproductive activity in mice is controlled by the oestrous cycle, which lasts 4-5 days. During this time, the hypothalamus mediates the release of gonadotropic hormones from the anterior pituitary that act on the ovary to control mating, ovulation, fertilization and luteinisation. This is followed by ovarian secretion of the major pregnancy steroid hormones oestrogen and progesterone, which support establishment and maintenance of pregnancy in case of successful fertilization. They also provide feedback to the hypothalamic-pituitary system to secrete the appropriate amount of pituitary gonadotropins in a

Development (2017) 144, 3264-3277 doi:10.1242/dev.155473

**Fig. 2. *Kdm4a*$^{-/-}$ females display low implantation rates and impaired pre-implantation embryos.** (A) The mean number (with s.d.) of oocytes flushed from *Kdm4a*$^{+/+}$ and *Kdm4a*$^{-/-}$ females ($n$=3 each group) following PMSG and hCG treatment. (B) Plugged wild-type ($n$=43) and *Kdm4a*$^{-/-}$ ($n$=14) females following timed mating were removed from the breeding cages and terminated at 9.5 dpc. The mean percentage of females with evidence of implantation is presented with 95% confidence interval. Unpaired $t$-test was used to determine statistical significance. (C) Crosses were set up as indicated. The average percentage of implantation sites is shown (with s.d.) that contained embryos with normal or delayed development, or where the embryo was resorbed. The number of litters analysed for each cross is indicated. Statistical significance was determined using the Holm–Sidak method, without assuming a consistent s.d. (D) Top panel: Representative images of embryos at 9.5 dpc from wild-type (+/+) females that were crossed with wild-type or *Kdm4a*$^{-/-}$ males. The embryonic genotype is indicated in the top left of each image. Bottom panel: An entire litter of embryos from a *Kdm4a*$^{-/-}$ female is depicted (note: this female had six additional implantation sites containing resorbed embryos). Scale bar: 1 mm. (E) Representative images of embryos that were flushed from the oviducts of wild-type (+/+) and *Kdm4a*$^{-/-}$ females at 2.5 dpc. Abnormal embryos are highlighted with an asterisk. (F) The distribution of embryos flushed from wild-type ($n$=10) and *Kdm4a*$^{-/-}$ ($n$=9) oviducts at 2.5 dpc is presented (with s.d.) and significance at each stage determined using unpaired $t$-test. n.s., not significant.

rhythmic fashion. Ovarian function is key to early embryonic development. This HPG (hypothalamic-pituitary-gonad) axis in females controls all major secondary sexual characteristics and tightly regulates reproductive fitness (Bachelot and Binart, 2005).

To determine whether hormonal cycles were activated normally in *Kdm4a*$^{-/-}$ females, multiple virgin and sexually mature females were exposed to the dirty bedding material of a stud male (Whitten, 1956) before actually pairing each female with a stud male. We observed that successful mating took significantly longer in *Kdm4a*$^{-/-}$ females (Fig. 3B). Consistent with our previous observation (Fig. 1C), there was no significant difference in the total proportion of plugged females. However, there was a clear difference in the dynamics of mating.

Following successful mating (Fig. 3B), at 2.5 dpc the majority of the embryos were delayed as observed previously. By then there should be ample levels of pregnancy steroid hormones secreted by the ovaries to initiate cross-talk with the uterus in preparation of implantation (Cha et al., 2012). We extracted blood prior to sacrificing the mice to prepare serum samples for the analysis of circulating pituitary (Haavisto et al., 1993; van Casteren et al., 2000) and steroid (Nilsson et al., 2015) hormones. Additionally, of each female, one ovary was used for intra-ovarian steroid hormone profiling by gas chromatography – tandem mass spectrometry (GC-MS) (Nilsson et al., 2015). In this analysis, we found no significant difference between wild-type and *Kdm4a*$^{-/-}$ ovary homogenates for the major ovarian steroid hormones oestrogen (E2) and progesterone (P4) and oestrone (E1). However, we observed significantly reduced levels of testosterone (T) in *Kdm4a*$^{-/-}$ females (Fig. 3C). The role of testosterone in the development of male secondary sexual characteristics is better studied, and its reproductive function in the female is not clear. Nevertheless, the presence of relatively normal levels of the main pregnancy hormones suggests normal ovarian function in that aspect.

When we analysed the circulating hormone levels, we found decreased levels of circulating testosterone and progesterone (Fig. 3D). Although the decrease in testosterone levels was consistent with the correspondingly decreased ovarian levels, the reduced circulating progesterone was in contrast to its normal levels in the ovary. This could be due to changes in progesterone metabolism post secretion. Although the role of progesterone in reproduction is well-known (Lydon et al., 1995), previous work suggests that even 25% of normal physiological levels is sufficient to support pre-implantation development and implantation (Milligan and Finn, 1997), leading us to speculate that *Kdm4a*$^{-/-}$ females retain sufficient amounts of progesterone to facilitate implantation.

Following stimuli from the central nervous system (CNS) through the hypothalamus, the pituitary secretes gonadotropins destined for the ovary that play a key role in female fertility. FSH (follicle-stimulating hormone), which controls folliculogenesis and ovulation, was not significantly altered (Fig. 3E). This is in agreement with our observations that *Kdm4a*$^{-/-}$ ovaries manifested all stages of folliculogenesis. *Kdm4a*$^{-/-}$ females had significantly reduced levels of luteinizing hormone (LH) (Fig. 3E), which in females regulates timing of oestrous, ovulation, and development and maintenance of the ovarian corpus luteum in females, thereby playing a crucial role in establishment of pregnancy (Ma et al., 2004; Kumar, 2007). Also, *Kdm4a*$^{-/-}$ females had reduced levels of prolactin (PRL) (Fig. 3E), which, along with its receptor (Prlr), plays a key role in female fertility as its absence results in lack of implantation and termination of pregnancy at the pre-implantation stage (Horseman et al., 1997; Ormandy et al., 1997).

Finally, we performed gene expression analysis on the frozen ovaries from these animals for major components of steroidogenesis pathway members (Hakkarainen et al., 2015). Although there was widespread biological variation between the animals, we found a trend towards increased expression of *Lhr* (*Lhcgr*), *Ar* and *Prlr*, but not of *Fshr* (Fig. S5). This upregulation could be a mechanism by which the mice compensate for the reduced circulating levels of the respective hormones. Taken together, we have demonstrated that Kdm4a expression is required for normal implantation despite its loss leading to only minor changes in the levels of pregnancy-related steroid hormones in the ovary.

### Kdm4a is required to maintain a uterine environment conducive for embryo implantation

We observed normal hormone synthesis in the ovary post-fertilization, but altered levels of circulating progesterone and pituitary hormones. Therefore, we investigated the effect of deleting *Kdm4a* on gene expression in the four major tissues of the HPG axis – the hypothalamus, ovary, oviduct and uterus at 2.5 dpc (Table S2). In the hypothalamus and pituitary, we found few expression changes, and none of the altered genes has previously been associated with fertility defects. Importantly, the expression of the precursor genes for LH and PRL, *Lhb* and *Prl* (expressed and secreted from discrete cells of the anterior pituitary), were not significantly altered, suggesting that their lower circulating levels are not linked to direct transcriptional control by Kdm4a.

However, loss of *Kdm4a* in 2.5 dpc ovaries led to 61 downregulated and 25 upregulated genes. Gene ontology (GO) analysis revealed that the downregulated genes were enriched for those involved in reproductive development processes, such as *Fshr*, *Kit*, *Taf4b*, *Oca2* and *Akr1c18* (20-alpha-HSD) (Fig. S6A). However, *Kdm4a*$^{-/-}$ female mice ovulate and fertilize eggs normally and normal post-ovulatory production of oestrogen and progesterone suggests these gene expression changes were not linked to the observed impact on pre-implantation development.

The uterus is a complex tissue of many cell types including the epithelium, stroma and myometrium. As the pre-implantation embryo transits towards the uterus, its first point of contact is the receptive endometrium, which is composed of luminal epithelium (LE) and glandular epithelium (GE). Whereas the LE mediates receptivity and blastocyst attachment, the GE enables synthesis and

Development (2017) 144, 3264-3277 doi:10.1242/dev.155473

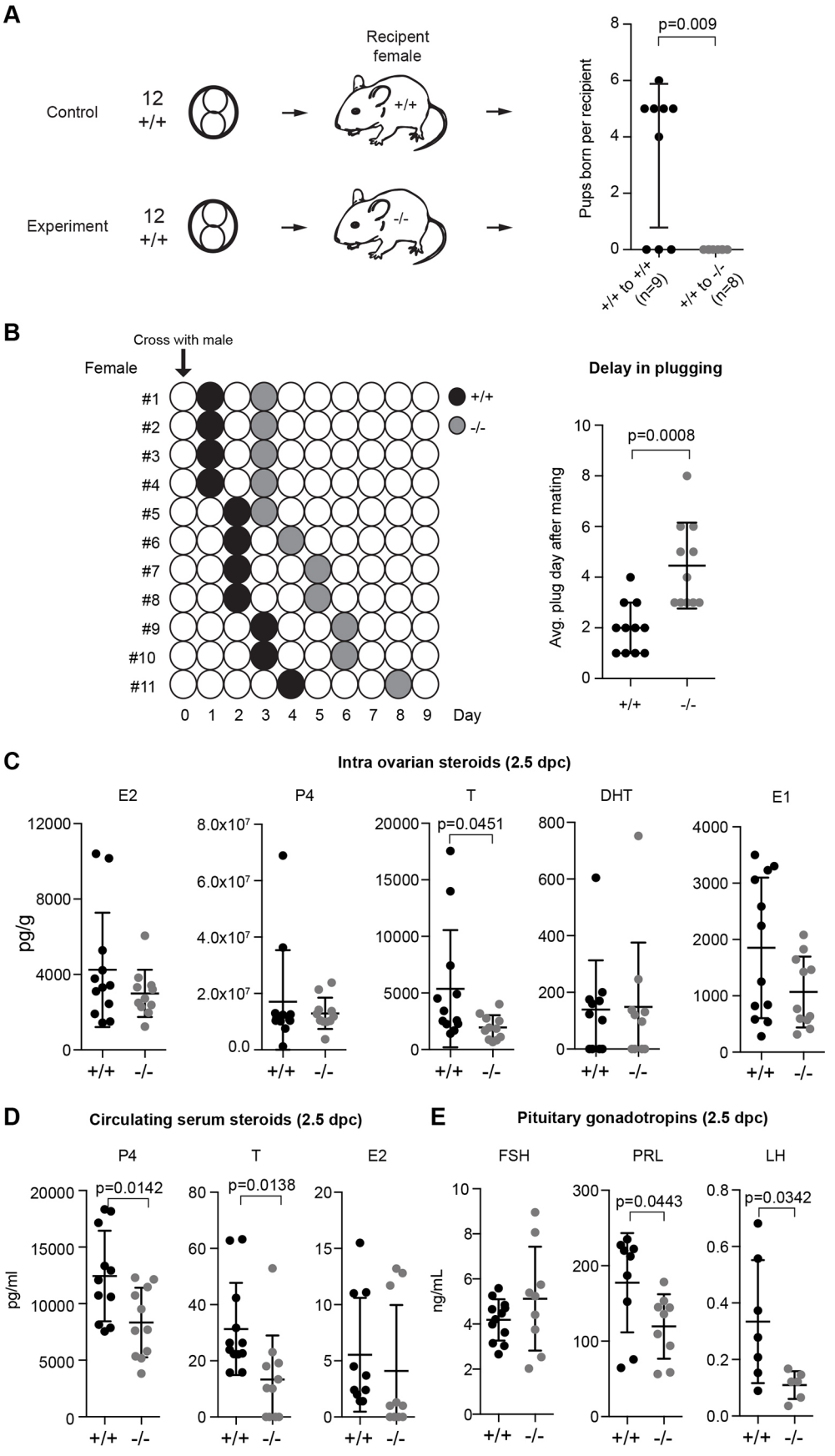


**Fig. 3. *Kdm4a* is required in the maternal reproductive tract to establish pregnancy.** (A) Scheme showing the transfer of 12 wild-type two-cell embryos into wild-type ($n$=9) or *Kdm4a*$^{-/-}$ ($n$=8) recipients. The average number (with s.d.) of pups per recipient is presented. Statistical significance was determined with Fisher's exact test. (B) Wild-type ($n$=11) and *Kdm4a*$^{-/-}$ ($n$=11) virgin 8- to 10-week-old females were set up for timed mating with wild-type males (indicated day 0 with arrow) following exposure to dirty bedding of stud male. The time of plug appearance is indicated with filled black and grey circles for wild-type (+/+) and *Kdm4a* knockout (–/–) females, respectively. Significance for delay in the number of days (with s.d.) taken to mate between the two groups was determined with an unpaired $t$-test. (C) Average concentration (with s.d.) of the indicated intra-ovarian steroid hormones as measured by GC-MS. Each measurement from an individual mouse is represented as an individual data point. (D) Average concentration (with s.d.) of the indicated circulating steroid hormones in serum as measured by GC-MS. Each measurement from an individual mouse is represented as an individual data point. (E) Average concentration (with s.d.) of circulating pituitary hormones in serum as measured by ELISA. Each measurement from an individual mouse is represented as an individual data point. Samples for C-E were collected from wild-type (+/+) and *Kdm4a* knockout (–/–) females during pregnancy at 2.5 dpc and significance determined with unpaired $t$-test. DHT, dihydrotestosterone; E1, oestrone; E2, oestrogen; P4, progesterone; T, testosterone.

Development (2017) 144, 3264-3277 doi:10.1242/dev.155473

transport of biomolecules that complete the implantation process with stromal decidualization. In *Kdm4a*$^{-/-}$ uteri, we found 151 downregulated and 169 upregulated genes ($\log_2$ FC±0.75, FDR<0.01). GO analysis revealed that most of the downregulated genes were predominantly linked to ion transport (including *Slc5a5*, *Slc13a5*, *Slc1a1*, *Fxyd4*, *Aqp11*), metabolic processes (including *Stard5*, *B3gnt5*, *Chst10*, *Cyp11a1*, *Cyp1b1*) and signal receptors (including *Csf2ra*, *Ptger2*, *Chrm4*, *Cadm3*) (Fig. 4A, Fig. S6B).

At 2.5 dpc, the uterus is in the pre-receptive stage and expresses certain genes that are highly enriched in the LE or GE, essentially forming a gene expression signature for these compartments (Filant and Spencer, 2013). We found that 35% (53/151) of the top downregulated genes overlap with those enriched in the LE, but not in the GE (Fig. 4B, Fig. S6C). On the other hand, only 7.5-8.5% of upregulated genes were enriched in either the LE or GE (Fig. 4B, Fig. S6C). This suggests that Kdm4a could have a general function in the LE. Indeed, loss-of-function studies on LE-enriched genes that are downregulated in *Kdm4a*$^{-/-}$ uteri, such as *Chst10* and *Ptger2*, have shown that they affect female fertility, particularly implantation rates and pre-implantation development of embryos in the tract (Suzuki-Anekoji et al., 2013; Kennedy et al., 1999).

Only upon the combined deletion of Kdm4 demethylases, are there observable changes in the global levels of H3K4me3 and H3K9me3 (Pedersen et al., 2016; Agger et al., 2016). To test whether loss of Kdm4a in the uterus would lead to changes in H3K4me3 and H3K9me3 levels, we performed chromatin immunoprecipitation followed by sequencing (ChIPSeq) in whole uterus at 2.5 dpc. As previously reported (Pedersen et al., 2016), Kdm4a is localized primarily to H3K4me3 positive transcription start-sites (TSSs). We did not observe global changes in H3K9me3 or H3K4me3 levels at TSSs as a result of Kdm4a deficiency (Fig. 4C), nor at most of the top downregulated genes. This might be due to dilution of the signal from more abundant uterine cell types compared with the LE cells in which the gene expression changes occur.

Despite this, we found among the downregulated genes *Csf2ra* – the unique binding receptor for the cytokine Csf2 (Table S1). Upon dimerization with its beta subunit *Csf2rb*, the combined signalling of Csf2, Il3 and Il5 is achieved (Hamilton, 2008). *Csf2ra* is expressed on the surface of the early embryo and on the maternal side expression peaks in the uterine stromal cells surrounding the LE post-mating. Csf2ra signalling plays a beneficial role in female fertility and regulates maternal cytokine signalling in the tract (Sferruzzi-Perri et al., 2009; Robertson et al., 2001, 1999; Jasper et al., 2000). We observed strong binding of Kdm4a across the *Csf2ra* gene, which is in agreement with a broad H3K4me3 'peak' at the large CpG-island. Consistent with a role for Kdm4a in maintaining sufficient levels of Csf2ra expression, loss of Kdm4a led to an increase in H3K9me3 levels and reduction of H3K4me3 (Fig. 4D). These changes were validated by ChIP-qPCR (Fig. 4E) and gene expression analysis by qPCR (Fig. 4F). Probably, the higher abundance of stromal cells allowed us to observe the changes of H3K4me3 and H3K9me3 associated with *Csf2ra*. These results suggest that *Csf2ra* is an example of a Kdm4a target gene that has an important role in regulating the normal uterine function. In summary, our results show that Kdm4a is important for normal uterine function, providing a maternal environment conducive for timely development and progression of early embryos.

### Kdm4a intrinsically exerts maternal-effect lethality on embryos

As *Kdm4a* is highly expressed in the oocyte, we wanted to investigate whether it could operate as a maternal effect gene influencing development of the early embryo. However, as loss of *Kdm4a* gives a clear maternal tract phenotype, we chose to address this hypothesis first *in vitro* by taking advantage of the fact that pre-implantation embryos can be easily cultured *in vitro* in simple media conditions until the blastocyst is ready for implantation (Richter, 2008). In particular, we wanted to understand how we could separate the roles of inherited mRNA/protein and endogenous embryonic *Kdm4a* in aiding normal pre-implantation development.

To address the role of Kdm4a in early embryogenesis, we set up different genetic combinations (Fig. 5A): (1) wild-type female mice paired with wild-type or *Kdm4a*$^{-/-}$ male mice (controls for normal development); (2) *Kdm4a*$^{-/-}$ female mice paired with wild-type male mice (maternal mutants – no inherited protein but endogenous copy of *Kdm4a* from father); and (3) *Kdm4a*$^{-/-}$ female mice paired with *Kdm4a*$^{-/-}$ male mice (maternal zygotic mutant – no inherited or endogenous copy of *Kdm4a*).

In the first instance, we set up natural timed mating of at least three females per condition with males of the appropriate genotype. Zygotes were isolated at 0.5 dpc upon observation of vaginal plug. Then we cultured embryos *in vitro* until 4.5 dpc in standard conditions to observe whether they formed cavitated blastocysts (Fig. 5B). As expected, a similar proportion (~80%) of wild-type oocytes fertilized with wild-type or *Kdm4a*$^{-/-}$ sperm proceeded to form healthy-looking blastocysts (Fig. 5B, left top and bottom panels; Fig. 5C). Maternal zygotic mutants had the lowest rate (~30%) of blastocyst development with a majority of resulting blastocysts of poor quality (Fig. 5B, lower right panel; Fig. 5C). Interestingly, the presence of a functional *Kdm4a* allele in the sperm improved the outcome with 50% of embryos forming blastocysts (Fig. 5B, upper right panel; Fig. 5C). These results indicate that *Kdm4a* can intrinsically affect the pre-implantation developmental potential of embryos through a maternal-zygotic effect.

In a second approach, we cultured control and maternal zygotic mutant embryos following *in vitro* fertilization (Fig. 5D). As the mutants undergo developmental defects, we wanted to quantify the cellularity of embryos. Both groups had comparable fertilization rates. For each day of culture, between 10 and 20 randomly picked embryos were fixed and stained with DAPI to visualize nuclei. Mutant embryos develop synchronously until the morula stage, after which there was extensive developmental arrest. Whereas control embryos progressed to form blastocysts on day 4, the majority of mutants had arrested between the 8- and 16-cell stage (Fig. 5D,E).

We next sought to validate our results *in vivo*. Wild-type and *Kdm4a*$^{-/-}$ oocytes were fertilized with *Kdm4a*$^{-/-}$ sperm as we have established normal fertility in these males. The resultant two-cell embryos were equally mixed and bilaterally transferred into pseudopregnant recipient mice (Fig. 5F, Fig. S7A,B). At 17 dpc, we performed a Caesarean section and genotyped the resultant foetuses. All seven recipient mice were pregnant with five of them harbouring at least six late-stage foetuses. Of the 45 foetuses retrieved in total, we identified only 13 mutants, which included four dead foetuses (mortality rate of 25%). The 32 control foetuses included three dead (mortality rate of 9%). Hence, *Kdm4a* maternal zygotic knockout embryos displayed a higher mortality rate and could not compete effectively with healthy embryos for implantation, establishing *Kdm4a* as a maternal effect gene. Taken together, our results show that the low implantation rates observed in *Kdm4a*$^{-/-}$ females are the result of deficiencies in both the mother and in the embryo.

Development (2017) 144, 3264-3277 doi:10.1242/dev.155473

A

| Genes downregulated in Kdm4a$^{-/-}$ uterus (151 genes) | |
|---|---|
| **GO biological process** | **count** |
| Organic anion transport | 10 |
| Anion transport | 12 |
| Lipid metabolic process | 16 |
| Transmembrane transport | 17 |
| Transmembrane transporter activity | 18 |
| Transporter activity | 19 |
| Small molecule metabolic process | 20 |
| Intrinsic component of plasma membrane | 20 |
| Organonitrogen compound metabolic process | 21 |
| Ion transport | 23 |

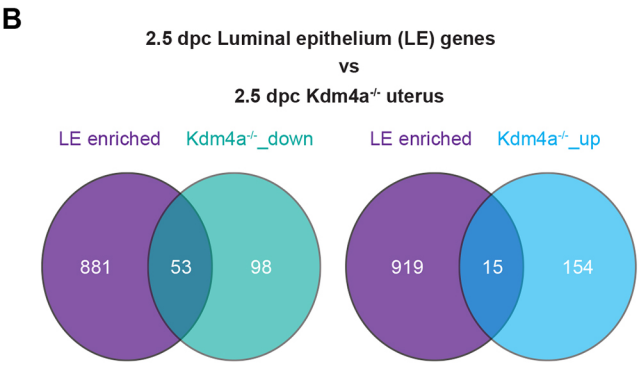


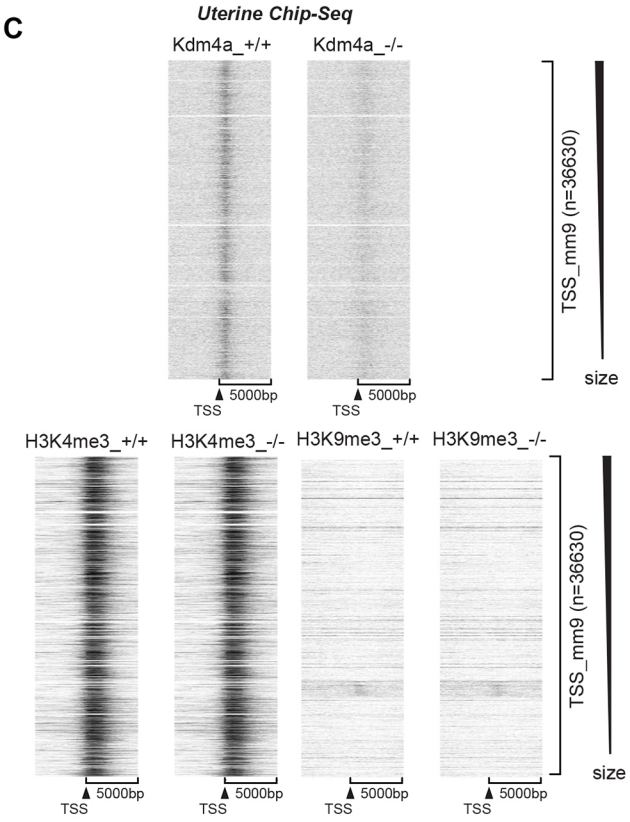


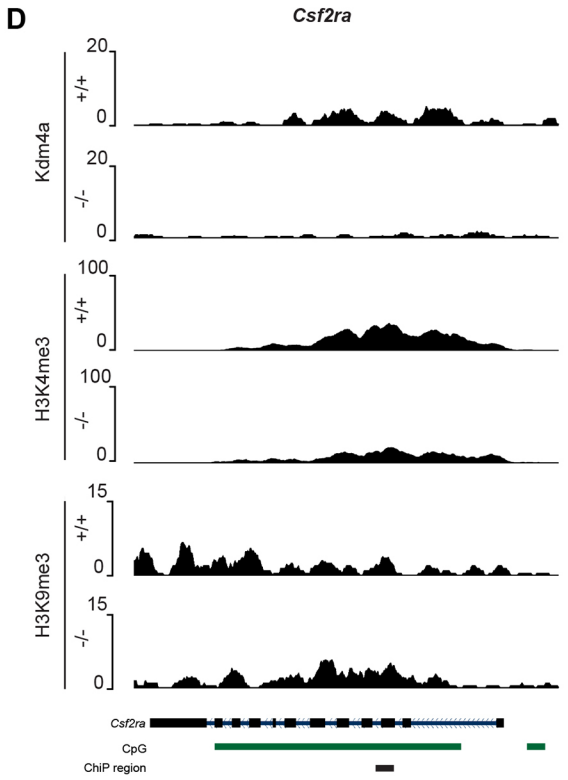


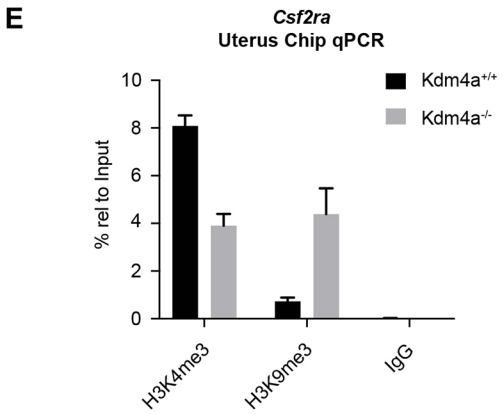


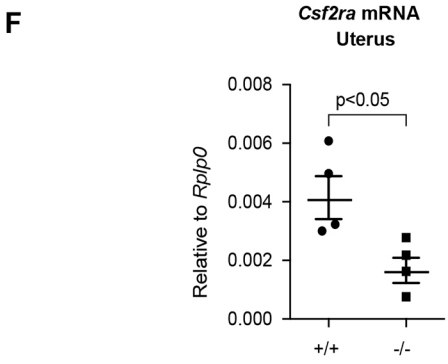


**Fig. 4.** See next page for legend.

Development (2017) 144, 3264-3277 doi:10.1242/dev.155473

**Fig. 4. *Kdm4a* affects maternal cytokine signalling in the uterus during early development.** (A) Gene ontology (GO) analysis for processes affected by loss of *Kdm4a* in the uterus focusing on downregulated genes identified by RNASeq between wild-type and *Kdm4a*$^{-/-}$ animals (*n*=3/group). (B) Overlap of published uterine luminal epithelium (LE)-enriched genes at 2.5 dpc with genes that were downregulated or upregulated in the *Kdm4a*$^{-/-}$ uterus as revealed in A. (C) ChIPSeq heatmap of Kdm4a, H3K4me3 and H3K9me3 binding in control and *Kdm4a*$^{-/-}$ uterus. A window size of 10,000 bp was chosen, centred around transcription start sites (TSSs). The regions were sorted in descending order of size and generated using EaSeq software. (D) Screen shots of Kdm4a, H3K4me3 and H3K9me3 enrichments at the *Csf2ra* locus. CpG islands are highlighted as green bars and the region evaluated by ChIP-qPCR is indicated with a black bar. (E) ChIP-qPCR experiments of H3K4me3, H3K9me3 and IgG (negative control) enrichments at *Csf2ra* in wild-type and Kdm4a$^{-/-}$ uterine tissue (with s.d.). (F) RT-qPCR for mean *Csf2ra* mRNA (with s.d.) in the 2.5 dpc uterus showing significant downregulation in the *Kdm4a*$^{-/-}$ females. Each data point represents one animal and is the average of technical replicates. Significance was determined using unpaired *t*-test.

## DISCUSSION

Here, we have demonstrated that the histone demethylase Kdm4a is essential for female, but not male, fertility. Mutant females produce similar numbers of embryos, but display poor implantation rates despite normal ovarian production of major pregnancy hormones oestrogen and progesterone. A comprehensive gene expression analysis revealed maximal gene expression changes in the uterus, suggesting a general uterine function for Kdm4a. Among downregulated genes, there was an overlap with genes enriched in the LE, which mediates uterine receptivity and blastocyst attachment. The identification of this strong association despite the complexity of the tissue present in the sample suggests that Kdm4a has an important role in regulating LE function. Owing to the overall contribution of the LE to the uterus, the changes in histone states at affected genes are diluted by more abundant uterine cell types. Although we did not observe global changes in H3K4 or H3K9 tri-methylation upon deletion of *Kdm4a*, we identified the cytokine receptor *Csf2ra* as being under direct control of Kdm4a. Csf2ra dimerizes with Csf2rb to mediate Csf2 (GM-CSF), Il3 and Il5 signalling (Hamilton, 2008). Csf2ra expression peaks post-mating within the stromal compartment of the uterus just surrounding the LE (Robertson et al., 2000b). As Csf2 is known to be secreted by endometrial cells in the uterus in response to mating stimuli (Sanford et al., 1992), reduced Csf2ra expression can locally impact maternal cytokine signalling in the tract. For instance, Il5-deficient mice have abnormal oestrous cycles and placental weights, even if no impact on implantation has been reported (Robertson et al., 2000a). As Csf2ra can mediate Il5 signalling, this could contribute in part to the delay in mating observed in *Kdm4a* null mice. Presently, *Csf2ra* knockout mice have not been described, and it is therefore not possible to make a side-by-side comparison of the functional consequences of losing Kdm4a and Csf2ra. However, we speculate that the reduced expression of Csf2ra through its effect on several signalling pathways at least partly contributes to the strong impact on female reproductive outcomes in the *Kdm4a*$^{-/-}$ mice.

Our results also show that Kdm4a has an intrinsic function in the oocyte and pre-determines the fate of a significant proportion of embryos as a maternal effect protein. Intriguingly, multiple studies recently revealed that murine oocytes uniquely harbour broad H3K4me3 domains in both promotors and intergenic regions that are actively remodelled as early embryo development proceeds (Vaquerizas and Torres-Padilla, 2016). As our current understanding of Kdm4a function places the protein at H3K4me3-positive promotors in somatic cells, this might in oocytes extend to intergenic regions to prevent widespread H3K9me3 gain. First, Kdm4a may be necessary in oocytes for sufficient transcription of key genes that are part of the build-up of maternal factors and RNAs prior to transcriptional arrest during meiotic prophase. For example, the maternal effect gene *Khdc3* (also known as *FILIA*) (Zheng and Dean, 2009) is among the top downregulated genes upon combined loss of Kdm4a/c in mESCs (Pedersen et al., 2016). Khdc3 is known to regulate genomic stability in mESCs (Zhao et al., 2015) and similar de-regulation in the oocyte could contribute to the developmental arrest we observe following *Kdm4a* deletion. Moreover, *Csf2ra* is expressed on the surface of early pre-implantation embryos, where it promotes glucose transport and blastomere viability by binding to Csf2 secreted from the uterus (Robertson et al., 2001). Apart from transcription, Kdm4a might also have a less-defined role in chromatin compaction, which is important for meiotic segregation and mitotic DNA replication timing during cleavage divisions in embryos and eventual embryonic genome activation (ZGA). Future studies are required to obtain further insights into Kdm4a function, which should include single-cell analysis and sequencing of wild-type and Kdm4a mutant cells. Interestingly, increased levels of Kdm4a have been shown to affect replication timing in an enzyme-dependent manner (Black et al., 2010), whereas it regulates DNA-damage response (DDR) in an enzyme-independent manner (Mallette et al., 2012). Both processes present conceptually important mechanisms to ensure early cell identity in the absence of any major transcription such as in an oocyte or early embryo (Egli and Le Bin, 2013). Recently, overexpression of KDM4 demethylase mRNAs dramatically rescued major embryonic developmental arrest following SCNT of murine and human oocytes (Chung et al., 2015; Matoba et al., 2014), pointing to a rate-limiting role in transcriptionally silent oocytes for increased H3K9me3 in ensuring efficient cell division and DNA replication.

In conclusion, our data demonstrate a dual requirement of Kdm4a: (1) as a maternal effect gene in ensuring proper early pre-implantation embryo development, and (2) in maintenance of a proper uterine environment conducive for embryonic progression and implantation.

## MATERIALS AND METHODS

### Generation of *Kdm4a* null mice

The generation of *Kdm4a* null mice was recently described (Pedersen et al., 2016). Mice were maintained on a C57Bl/6 background. $\chi^2$ tests were used to obtain *P*-values for the observed genotypic distributions. Analysis of survival curves was performed with a log-rank test in GraphPad Prism. Mouse breeding pairs were housed in conventional cages behind a specific pathogen-free barrier and experimental mice were housed in groups at the University of Copenhagen in individually ventilated cages. All animals were exposed to 12 h of light (06:00 to 18:00 h) and had free access to water and a standard mouse chow diet. All mouse work was approved by the Danish Animal Ethical Committee (Dyreforsøgstilsynet).

### Timed matings and embryo analysis

All males used for breeding were previously confirmed to be fertile. Weaned control and knockout females were housed together until 8 weeks of age to control for pheromone exposures. Oestrus cycle was activated by exposing females to male hormones by moving the animals for 2 days into a cage with dirty bedding material from a cage where a stud male had been housed. Afterwards, 1:1 breeding with stud males was set up and females were monitored every morning for vaginal plug formation. For super-ovulation, immature females of 4 weeks of age were treated following a standard protocol: intra-peritoneal administration of 5 IU pregnant mare's serum gonadotropin (PMSG) per female and, 47 h later, 5 IU human chorionic gonadotrophin (hCG) per female. Afterwards, they were crossed 1:1 with

Development (2017) 144, 3264-3277 doi:10.1242/dev.155473

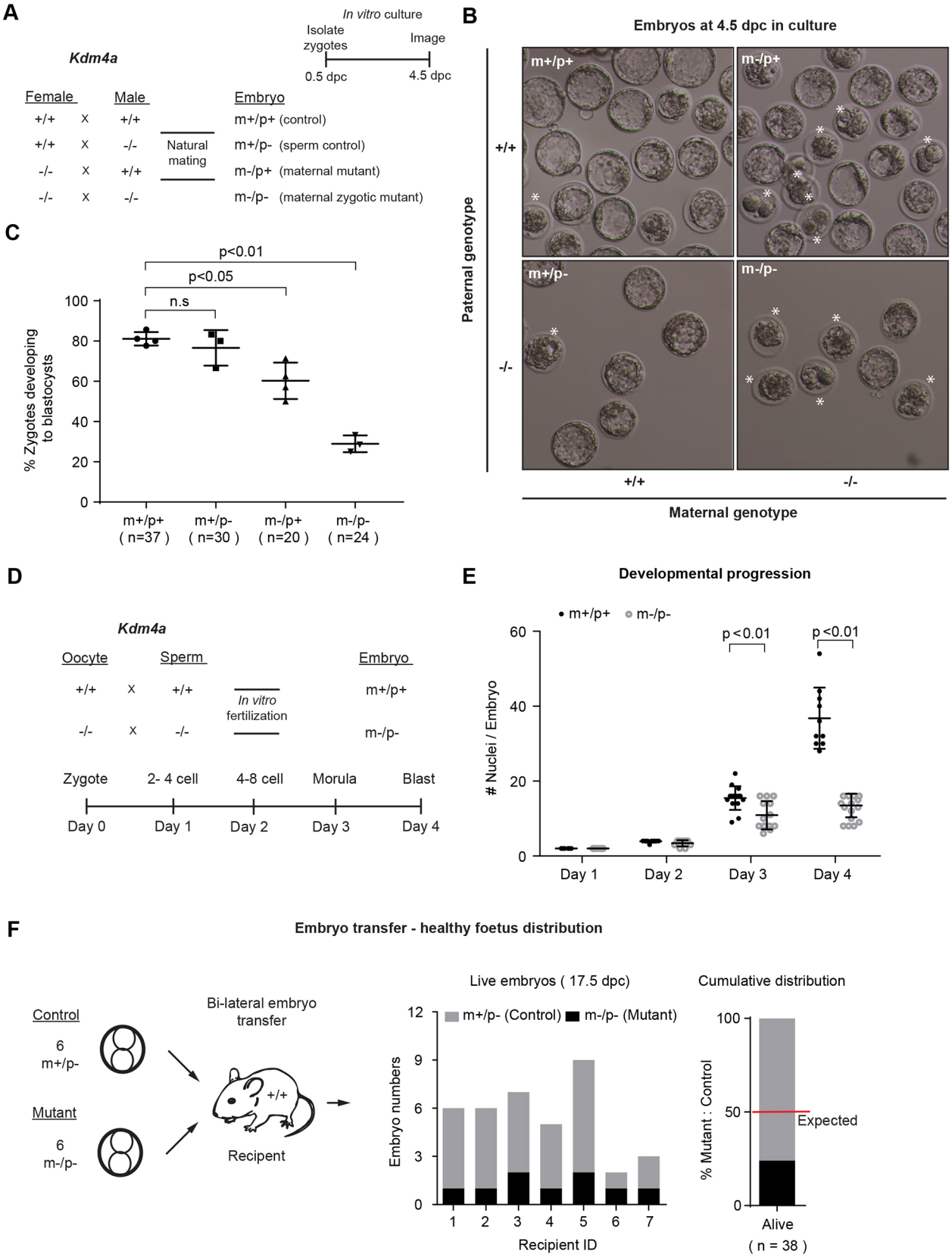


**Fig. 5.** See next page for legend.

stud males. The morning of vaginal plug detection was always considered 0.5 dpc. Zygotes for *in vitro* culture were isolated at 0.5 dpc, cultured in KSOMaa Evolve medium (LifeGlobal group) micro-drops covered by mineral oil (Sigma-Aldrich) and imaged every day. Morulae were flushed out of the oviduct at 2.5 dpc using M2 medium (Sigma-Aldrich). For embryo transfer experiments, two-cell embryos were isolated at 1.5 dpc and

Development (2017) 144, 3264-3277 doi:10.1242/dev.155473

**Fig. 5. *Kdm4a* intrinsically affects embryo development as a maternal-zygotic gene.** (A) Mating scheme and strategy to compare developmental outcomes in culture between control and maternal *Kdm4a* knockout embryos. (B) Representative images of embryos at 4.5 dpc after culture for 4 days following isolation at 0.5 dpc. The genotypes of the sperm and oocyte are highlighted along the *y*- and *x*-axes, respectively. Delayed/poor quality embryos are highlighted with asterisks. (C) Comparison of the mean percentage of zygotes (with s.d.) resulting in healthy-looking blastocysts in culture. Statistical significance between the experimental group with control (m+/p+) was performed using *t*-test. Each data point represents one female with at least three females per group (*n*=number of total embryos derived per group). (D) Scheme for *in vitro* fertilization and culture of wild-type and *Kdm4a*$^{-/-}$ oocytes with appropriate sperm genotype (left panel). (E) The mean number of nuclei (with s.d.) observed per embryo following each day of culture is compared between m+/p+ and m−/p− embryos using an unpaired *t*-test where each data point represents one embryo. (F) Bilateral two-cell embryo transfer of wild-type (control) and *Kdm4a* knockout eggs fertilized *in vitro* by knockout sperm into wild-type recipient mice (7 in all) delivered at 17.5 dpc by C-section. Control and mutant embryos were mixed in 1:1 ratio and 12 embryos were transplanted into each oviduct. Graphs represent the number of live embryos found per recipient as well as cumulative genotype distribution as a percentage with mutants in black and controls in grey. n.s., not significant.

transferred into the oviduct of 0.5 dpc pseudo-pregnant recipient females the same day, according to standard procedure. For analysis of mid- to late gestation embryos, plugged females were sacrificed through cervical dislocation and embryos dissected in cold PBS before imaging with a dissection light microscope (Leica). All animals were re-genotyped after sacrifice to confirm identity.

### β-Galactosidase assay

Embryos and tissues were subjected to whole mount β-galactosidase staining. Samples were fixed in 0.25% glutaraldehyde in PBS for 5-30 min (with longer incubation times for larger samples), washed in PBS and stained in 20 mM Tris-HCl pH 7.4, 2 mM $MgCl_2$, 0.02% Igepal CA-630, 0.01% sodium deoxycholate, 5 mM potassium ferrocyanide and 5 mM potassium ferricyanide. Following overnight post-fixation with 4% paraformaldehyde (PFA) at 4°C, embryos and tissues were cleared with 1% KOH containing an increasing glycerol gradient (Schatz et al., 2005).

### Establishment of mouse embryonic stem cells

Tissue culture grade 24-well plates (Fisher Scientific, 142475) were coated with 0.1% gelatin (Sigma, G9391) at 37°C. Pre-implantation embryos from control and *Kdm4a*$^{-/-}$ mice were isolated at 3.5 dpc and cultured overnight in KSOMaa Evolve medium (LifeGlobal group) to generate blastocysts. At 4.5 dpc, embryos were placed in individual wells of the gelatin-coated plates in mESC medium (2i-LIF condition) as described by Pedersen et al. (2016) to allow hatching and establishment of mESC lines. The generated cells lines were then tested to be negative for mycoplasma contamination.

### Gonadotropin and steroid measurements

Females were weighed and anaesthetized using an intra-peritoneal dose of 20 µg/µl Avertin (25 µl/g body weight). Blood was withdrawn from the retro-orbital sinus using heparinized capillaries and transferred to 2 ml protein low-bind tubes (Eppendorf). Serum was prepared from blood as described previously (Hakkarainen et al., 2015). For intra-ovarian steroid profiling, one ovary per female was collected and immediately flash frozen in liquid nitrogen. LH, PRL and FSH were measured by dissociation-enhanced lanthanide fluorescence immunoassay (DELFIA) and intra-tissue ovarian steroid measurements were performed using gas chromatography tandem mass spectrometry method. Both methods were performed as described previously (Hakkarainen et al., 2015; Nilsson et al., 2015; Haavisto et al., 1993; van Casteren et al., 2000). Animals were re-genotyped post-sacrifice and the investigators measuring hormones were completely blinded to the genotypes until post-experiment data analysis.

### RNA extraction, RT-qPCR and gene expression analysis

Tissues were collected, flash frozen in liquid nitrogen and stored at −80°C. Tissues were homogenized using a Fisherbrand Disposable Pestle system in RLT+ buffer and RNA was extracted using RNeasy Plus Mini kit (Qiagen, 74136). Reverse transcription was performed with random hexamers using TaqMan RT reagents (Life Technologies, N8080234). For qPCR, Lightcycler 480 Sybr Green I Master mix (Roche, 04887352001) was used with 0.5 µM of each primer in a total volume of 10 µl/reaction. Primer sequences are listed in Table S3. The housekeeping gene *Rplp0* was used for normalization and all data are presented as mean±s.d. for biological replicates. For RNASeq, only RNA samples with a RIN quality score of eight or above were used to prepare libraries.

### RNASeq

For RNASeq analysis, tissue RNA quality was measured using an Agilent 2100 Bioanalyzer system (Agilent, G2940CA) and RNA 6000 Nano reagents (Agilent, 5067-1511). RIN scores were at least eight for samples used in the RNASeq with three biological replicates for each tissue. RNASeq libraries were generated using the TruSeq RNA Sample Prep Kit v2 (Illumina, RS-122-2001) and quantified using Qubit (Thermo Fisher Scientific, Q32851) and the Agilent 2100 Bioanalyzer system (Agilent, G2940CA). Libraries generated from each individual tissue were pooled to a final library of 1.8 picomolar (pM) concentration. This pooled library was subjected to 75 base pair (bp) single-end sequencing on an Illumina NextSeq500 platform followed by downstream analysis as described below. In the analysis of data, we used the following cut-offs: absolute fold change $\log_2(|FC|)>0.75$, $P<0.05$ and FDR<0.1.

### RNASeq differential expression analysis pipeline

RNASeq data were analysed using a Galaxy pipeline. Three biological replicates were used per tissue sample each from an independent animal at 2.5 dpc. Each animal was re-genotyped post-sacrifice to confirm its genetic identity. Briefly, sequenced files of each sample from multiple lanes were concatenated into one file using the 'concatenate' command. Concatenated files were converted into *fastqsanger* format and sequencing quality reports generated using *FastQC* tool. After confirming high sequencing quality, each sample was subjected to sliding window adaptor trimming using the *Trimmomatic* tool with an Illuminaclip step specific for TruSeq3 adaptor sequences. The output file was then aligned to the mm10 reference genome using *RNA-STAR* tool for single end sequencing using default parameters to generate the aligned **.bam* file output. The uniquely mapped reads were counted using *htseq-count* tool in union mode against the mm10 reference genome annotation using default parameters to generate the read counts with features. Finally, we measured differently expressed features from count tables between the three knockouts (Factor level 1) and controls (Factor level 2) samples using the *DeSeq2* tool using default parameters. This generated the list of differentially expressed genes with mean normalized read counts. Thresholds were placed for $\log_2$ fold change of 0.75 and adjusted *P*-value below 0.1 and the output files for all tissues is presented in Table S2.

### Chromatin immunoprecipitation

For tissue ChIP, ovaries from five mice were pooled for preparing chromatin. In the case of uteri, tissue from females aged 8-12 weeks were harvested and cut into halves. Fixation was performed for 10 min using 1% formaldehyde in PBS. Fixation was stopped using 0.125 M glycine and samples were washed twice with PBS. Chromatin preparation, immunoprecipitation (IP) and wash and elution were performed as described previously (Pedersen et al., 2016). For Kdm4a IP, 750 µg -1 mg chromatin was used per IP (300-1500 bp average size). For H3K4me3 and H3K9me3 histone IP, 40-100 µg chromatin was used per IP (100-300 bp average size). All steps were performed in conditions containing HALT protease inhibitor cocktail (Thermo Fisher Scientific, 78430). Two nanograms of IP DNA was used to generate ChiPSeq libraries using the NEBNext Ultra II DNA library prep kit (Illumina, E7645S) and quantified using Qubit (Thermo Fisher Scientific, Q32851) and the Agilent 2100 Bioanalyzer system (Agilent, G2940CA). Input DNA was used as negative control as IgG did not yield enough starting material to generate libraries.

Development (2017) 144, 3264-3277 doi:10.1242/dev.155473

1.8 pM of single end pooled library was loaded onto an Illumina NextSeq500 sequencing platform. For ChiP-RT qPCR, 1 µl of eluate IP DNA from two biological samples were measured in technical replicates.

### ChIPSeq data analysis pipeline

As for RNASeq, sequenced files of each sample were concatenated into one file using the 'concatenate' command. Concatenated files were converted into *fastqsanger* format and sequencing quality reports generated using *FastQC* tool. After confirming high sequencing quality, input samples were converted to Sanger formatting through *FastQ Groomer* tool. Files were adaptor trimmed using the *Cutadapt* tool. The output files were mapped to mm9 mouse genome build using *Bowtie* for single end Illumina sequencing to generate aligned *.*bam* files. Bam files were converted into bedgraph files using *BAM to BED* tool. Bedgraph files were used as input files for ChIPSeq analysis using the open access EaSeq software (Lerdrup et al., 2016).

TSSs were extracted as a region set from the 'refFlat_mm9_2017-02-10' gene set based on the annotated positions ranging from the start of 0 with an offset of −1500 bp to start of 0 with an offset of 500 bp. Regions larger than 100 million bp or smaller than 100 were set to those sizes. Non-canonical genes (those containing '_' in their name) were excluded.

For H3K4me3 and H3K9me3 ChIPSeq, unique reads from two biological replicates for each genotype were pooled and shrunk to 25 and 12.9 million randomly selected reads, respectively, for comparison. For Kdm4a ChIPSeq, unique reads from wild-type (pooled from two biological replicates) and knockout (one sample) samples were shrunk to 13.6 million randomly selected reads and compared directly. Heat maps and filled tracks were generated as described in the software tutorials available online http://easeq.net/.

### Immunohistochemistry

After harvesting, tissues were immediately placed in 4% PFA overnight and transferred to 70% ethanol the next morning. The tissues were then embedded in paraffin blocks and 4 µm sections transferred to SuperFrostPlus slides (Thermo Fisher Scientific). For each experiment, slides were de-paraffinized, hydrated and subjected to antigen retrieval using freshly prepared 10 mM sodium citrate with 0.05% Tween (pH 6), following primary antibody incubation according to the supplier's instructions. Sections were then quenched with 0.3% hydrogen peroxide, incubated with polyclonal goat anti-rabbit immunoglobulins/HRP (DAKO, P0448) antibody, and the colour development was performed using NovaRed (Vector Laboratories, SK-4800). Quantification of Ki67- and Caspase 3-positive staining across whole tissue sections was performed using ImageJ software as described under http://imagej.net/Particle_Analysis. Control and knockout tissue samples were subjected to the same threshold values in all cases.

### Nuclei counts of *in vitro* cultured embryos

Embryos were fixed in 4% PFA at room temperature for 20 min. They were then blocked and permeabilized in PBS supplemented with 1% bovine serum albumin (BSA) and 0.5% Triton X-100 for 1 h and washed three times in PBS supplemented with 1% BSA. Then the embryos were incubated for 5 min in DAPI (50 µg/ml) and washed again three times in PBS supplemented with 1% BSA. After a final wash in miliQ water, the embryos were mounted in Vectashield mounting medium with DAPI with a coverslip and sealed with nail varnish. Slides were kept overnight at room temperature in the dark and transferred to 4°C for storage until imaging. *z*-stack images were acquired using Leica SP8 confocal microscope covering the entire embryo and were used to count nuclei present in each embryo. For each day of culture, at least 15-20 embryos were fixed and analysed.

### Antibodies

Antibodies used in immunohistochemistry: anti-Caspase 3 (1:200, Cell Signaling Technology, 9661), anti-Ki67 (1:200 Leica, NCL-Ki67p), anti-Kdm4a (1:100, Cell Signaling Technology, 5328). Antibodies used in ChipSeq: the Kdm4a (5 µg/ml IP, Cell Signaling Technology, 5328), H3K4me3 (5 µg/ml IP, Cell Signaling Technology, 9751) and H3K9me3 (2 µg/ml IP, Abcam, ab8898) antibodies used were the same as reported previously (Pedersen et al., 2016). The substrate specificity of antibodies recognizing modified histones was confirmed previously with an ELISA assay using a histone peptide library (Pedersen et al., 2014).

### Statistical analyses

Experiments were performed at least twice and with at least five or more biological samples included per experiment to allow for good sample size and statistics with individual data points plotted. Graphs are represented with individual data points in most cases and all error bars representing mean with standard deviation as a measure of indicating biological data variability. For qPCR data, only the average of technical replicates is plotted. Statistical analysis was performed using GraphPad Prism 6. The majority of the experiments involves two sample one-sided comparisons using *t*-tests to assess significant phenotypic differences between wild-type and $Kdm4a^{-/-}$ animals. Other methods to assess significance have been stated in the relevant figure legends. Differences with a *P*-value <0.05 or <0.01 were considered to be significant and highly significant, respectively.

#### Acknowledgements

We thank all members of the Helin laboratory for discussion, technical advice and support. We wish to acknowledge Karl Agger and Simon Weissman for expert advice, and Kasper Bonderup and Fengqin Jia for technical assistance.

#### Competing interests

The authors declare no competing or financial interests.

#### Author contributions

Conceptualization: A.S., S.M.K., K.H.; Methodology: A.S., S.M.K., J.M.G., C.O., M.P., K.H.; Formal analysis: A.S., S.M.K., C.O., M.P., K.H.; Investigation: S.M.K., J.M.G., C.O., M.P.; Writing - original draft: A.S., S.M.K., K.H.; Writing - review & editing: A.S., S.M.K., K.H.; Supervision: K.H.; Project administration: K.H.; Funding acquisition: K.H.

#### Funding

A.S. was supported by a PhD fellowship from the Initial Training Network, INGENIUM, funded by the FP7 Marie Curie Actions of the European Commission (FP7 MC-ITN INGENIUM project no. 290123). S.M.K. was supported by a postdoctoral fellowship from the Netherlands Organization for Scientific Research (Nederlandse Organisatie voor Wetenschappelijk Onderzoek, NWO; 825.10.027). This work was further supported by the Danish Cancer Society (Kræftens Bekæmpelse; DP08005), the Danish National Research Foundation (Danmarks Grundforskningsfond; DNRF 82), the Novo Nordisk Fonden (NNF 17CC0027852) and the Lundbeck Foundation (Lundbeckfonden; R140-2013-13595).

#### Data availability

RNASeq and ChIP-Seq data have been deposited at Gene Expression Omnibus under accession number GSE96686.

#### Supplementary information

Supplementary information available online at
http://dev.biologists.org/lookup/doi/10.1242/dev.155473.supplemental

#### References

**Agger, K., Miyagi, S., Pedersen, M. T., Kooistra, S. M., Johansen, J. V. and Helin, K.** (2016). Jmjd2/Kdm4 demethylases are required for expression of Il3ra and survival of acute myeloid leukemia cells. *Genes Dev.* **30**, 1278-1288.

**Bachelot, A. and Binart, N.** (2005). Corpus luteum development: lessons from genetic models in mice. *Curr. Top. Dev. Biol.* **68**, 49-84.

**Berry, W. L. and Janknecht, R.** (2013). KDM4/JMJD2 histone demethylases: epigenetic regulators in cancer cells. *Cancer Res.* **73**, 2936-2942.

**Berry, W. L., Shin, S., Lightfoot, S. A. and Janknecht, R.** (2012). Oncogenic features of the JMJD2A histone demethylase in breast cancer. *Int. J. Oncol.* **41**, 1701-1706.

**Black, J. C., Allen, A., Van Rechem, C., Forbes, E., Longworth, M., Tschöp, K., Rinehart, C., Quiton, J., Walsh, R., Smallwood, A. et al.** (2010). Conserved antagonism between JMJD2A/KDM4A and HP1gamma during cell cycle progression. *Mol. Cell* **40**, 736-748.

**Black, J. C., Manning, A. L., Van Rechem, C., Kim, J., Ladd, B., Cho, J., Pineda, C. M., Murphy, N., Daniels, D. L., Montagna, C. et al.** (2013). KDM4A lysine demethylase induces site-specific copy gain and rereplication of regions amplified in tumors. *Cell* **154**, 541-555.

Development (2017) 144, 3264-3277 doi:10.1242/dev.155473

**Brown, S. D. M. and Moore, M. W.** (2012). The international mouse phenotyping consortium: past and future perspectives on mouse phenotyping. *Mamm. Genome* **23**, 632-640.
**Cha, J., Sun, X. and Dey, S. K.** (2012). Mechanisms of implantation: strategies for successful pregnancy. *Nat. Med.* **18**, 1754-1767.
**Chen, Z., Zang, J., Whetstine, J., Hong, X., Davrazou, F., Kutateladze, T. G., Simpson, M., Mao, Q., Pan, C.-H., Dai, S. et al.** (2006). Structural insights into histone demethylation by JMJD2 family members. *Cell* **125**, 691-702.
**Chen, Z., Zang, J., Kappler, J., Hong, X., Crawford, F., Wang, Q., Lan, F., Jiang, C., Whetstine, J., Dai, S. et al.** (2007). Structural basis of the recognition of a methylated histone tail by JMJD2A. *Proc. Natl. Acad. Sci. USA* **104**, 10818-10823.
**Cheung, N., Fung, T. K., Zeisig, B. B., Holmes, K., Rane, J. K., Mowen, K. A., Finn, M. G., Lenhard, B., Chan, L. C. and So, C. W. E.** (2016). Targeting aberrant epigenetic networks mediated by PRMT1 and KDM4C in acute myeloid leukemia. *Cancer Cell* **29**, 32-48.
**Chin, Y.-W. and Han, S.-Y.** (2015). KDM4 histone demethylase inhibitors for anti-cancer agents: a patent review. *Expert Opin. Ther. Pat.* **25**, 135-144.
**Chung, Y. G., Matoba, S., Liu, Y., Eum, J. H., Lu, F., Jiang, W., Lee, J. E., Sepilian, V., Cha, K. Y., Lee, D. R. et al.** (2015). Histone demethylase expression enhances human somatic cell nuclear transfer efficiency and promotes derivation of pluripotent stem cells. *Cell Stem Cell* **17**, 758-766.
**Cloos, P. A. C., Christensen, J., Agger, K., Maiolica, A., Rappsilber, J., Antal, T., Hansen, K. H. and Helin, K.** (2006). The putative oncogene GASC1 demethylates tri- and dimethylated lysine 9 on histone H3. *Nature* **442**, 307-311.
**Dahl, J. A., Jung, I., Aanes, H., Greggains, G. D., Manaf, A., Lerdrup, M., Li, G., Kuan, S., Li, B., Lee, A. Y. et al.** (2016). Broad histone H3K4me3 domains in mouse oocytes modulate maternal-to-zygotic transition. *Nature* **537**, 548-552.
**Dimitrova, E., Turberfield, A. H. and Klose, R. J.** (2015). Histone demethylases in chromatin biology and beyond. *EMBO Rep.* **16**, 1620-1639.
**Egli, D. and Le Bin, G. C.** (2013). Tying replication to cell identity. *Nat. Rev. Mol. Cell Biol.* **14**, 326.
**Filant, J. and Spencer, T. E.** (2013). Cell-specific transcriptional profiling reveals candidate mechanisms regulating development and function of uterine epithelia in mice. *Biol. Reprod.* **89**, 86.
**Greer, E. L. and Shi, Y.** (2012). Histone methylation: a dynamic mark in health, disease and inheritance. *Nat. Rev. Genet.* **13**, 343-357.
**Haavisto, A. M., Pettersson, K., Bergendahl, M., Perheentupa, A., Roser, J. F. and Huhtaniemi, I.** (1993). A supersensitive immunofluorometric assay for rat luteinizing hormone. *Endocrinology* **132**, 1687-1691.
**Hakkarainen, J., Jokela, H., Pakarinen, P., Heikela, H., Katkanaho, L., Vandenput, L., Ohlsson, C., Zhang, F.-P. and Poutanen, M.** (2015). Hydroxysteroid (17beta)-dehydrogenase 1-deficient female mice present with normal puberty onset but are severely subfertile due to a defect in luteinization and progesterone production. *FASEB J.* **29**, 3806-3816.
**Hamilton, J. A.** (2008). Colony-stimulating factors in inflammation and autoimmunity. *Nat. Rev. Immunol.* **8**, 533-544.
**Hojfeldt, J. W., Agger, K. and Helin, K.** (2013). Histone lysine demethylases as targets for anticancer therapy. *Nat. Rev. Drug Discov.* **12**, 917-930.
**Horseman, N. D., Zhao, W., Montecino-Rodriguez, E., Tanaka, M., Nakashima, K., Engle, S. J., Smith, F., Markoff, E. and Dorshkind, K.** (1997). Defective mammopoiesis, but normal hematopoiesis, in mice with a targeted disruption of the prolactin gene. *EMBO J.* **16**, 6926-6935.
**Huang, Y., Fang, J., Bedford, M. T., Zhang, Y. and Xu, R. M.** (2006). Recognition of histone H3 lysine-4 methylation by the double tudor domain of JMJD2A. *Science* **312**, 748-751.
**Iwamori, N., Zhao, M., Meistrich, M. L. and Matzuk, M. M.** (2011). The testis-enriched histone demethylase, KDM4D, regulates methylation of histone H3 lysine 9 during spermatogenesis in the mouse but is dispensable for fertility. *Biol. Reprod.* **84**, 1225-1234.
**Jasper, M. J., Robertson, S. A., Van Der Hoek, K. H., Bonello, N., Brännström, M. and Norman, R. J.** (2000). Characterization of ovarian function in granulocyte-macrophage colony-stimulating factor-deficient mice. *Biol. Reprod.* **62**, 704-713.
**Kawazu, M., Saso, K., Tong, K. I., Mcquire, T., Goto, K., Son, D.-O., Wakeham, A., Miyagishi, M., Mak, T. W. and Okada, H.** (2011). Histone demethylase JMJD2B functions as a co-factor of estrogen receptor in breast cancer proliferation and mammary gland development. *PLoS ONE* **6**, e17830.
**Kennedy, C. R., Zhang, Y., Brandon, S., Guan, Y., Coffee, K., Funk, C. D., Magnuson, M. A., Oates, J. A., Breyer, M. D. and Breyer, R. M.** (1999). Salt-sensitive hypertension and reduced fertility in mice lacking the prostaglandin EP2 receptor. *Nat. Med.* **5**, 217-220.
**Klose, R. J., Yamane, K., Bae, Y., Zhang, D., Erdjument-Bromage, H., Tempst, P., Wong, J. and Zhang, Y.** (2006). The transcriptional repressor JHDM3A demethylates trimethyl histone H3 lysine 9 and lysine 36. *Nature* **442**, 312-316.
**Kooistra, S. M. and Helin, K.** (2012). Molecular mechanisms and potential functions of histone demethylases. *Nat. Rev. Mol. Cell Biol.* **13**, 297-311.
**Kumar, T. R.** (2007). Functional analysis of LHbeta knockout mice. *Mol. Cell. Endocrinol.* **269**, 81-84.
**Lerdrup, M., Johansen, J. V., Agrawal-Singh, S. and Hansen, K.** (2016). An interactive environment for agile analysis and visualization of ChIP-sequencing data. *Nat. Struct. Mol. Biol.* **23**, 349-357.
**Li, B.-X., Zhang, M.-C., Luo, C. L., Yang, P., Li, H., Xu, H.-M., Xu, H.-F., Shen, Y.-W., Xue, A.-M. and Zhao, Z.-Q.** (2011). Effects of RNA interference-mediated gene silencing of JMJD2A on human breast cancer cell line MDA-MB-231 in vitro. *J. Exp. Clin. Cancer Res.* **30**, 90.
**Li, B. X., Luo, C. L., Li, H., Yang, P., Zhang, M. C., Xu, H. M., Xu, H. F., Shen, Y. W., Xue, A. M. and Zhao, Z. Q.** (2012). Effects of siRNA-mediated knockdown of jumonji domain containing 2A on proliferation, migration and invasion of the human breast cancer cell line MCF-7. *Exp. Ther. Med.* **4**, 755-761.
**Liu, W., Liu, X., Wang, C., Gao, Y., Gao, R., Kou, X., Zhao, Y., Li, J., Wu, Y., Xiu, W. et al.** (2016). Identification of key factors conquering developmental arrest of somatic cell cloned embryos by combining embryo biopsy and single-cell sequencing. *Cell Discov.* **2**, 16010.
**Lydon, J. P., Demayo, F. J., Funk, C. R., Mani, S. K., Hughes, A. R., Montgomery, C. A., Jr, Shyamala, G., Conneely, O. M. and O'malley, B. W.** (1995). Mice lacking progesterone receptor exhibit pleiotropic reproductive abnormalities. *Genes Dev.* **9**, 2266-2278.
**Ma, X., Dong, Y., Matzuk, M. M. and Kumar, T. R.** (2004). Targeted disruption of luteinizing hormone beta-subunit leads to hypogonadism, defects in gonadal steroidogenesis, and infertility. *Proc. Natl. Acad. Sci. USA* **101**, 17294-17299.
**Mallette, F. A., Mattiroli, F., Cui, G., Young, L. C., Hendzel, M. J., Mer, G., Sixma, T. K. and Richard, S.** (2012). RNF8- and RNF168-dependent degradation of KDM4A/JMJD2A triggers 53BP1 recruitment to DNA damage sites. *EMBO J.* **31**, 1865-1878.
**Matoba, S., Liu, Y., Lu, F., Iwabuchi, K. A., Shen, L., Inoue, A. and Zhang, Y.** (2014). Embryonic development following somatic cell nuclear transfer impeded by persisting histone methylation. *Cell* **159**, 884-895.
**Milligan, S. R. and Finn, C. A.** (1997). Minimal progesterone support required for the maintenance of pregnancy in mice. *Hum. Reprod.* **12**, 602-607.
**Ng, S. S., Kavanagh, K. L., Mcdonough, M. A., Butler, D., Pilka, E. S., Lienard, B. M. R., Bray, J. E., Savitsky, P., Gileadi, O., Von Delft, F. et al.** (2007). Crystal structures of histone demethylase JMJD2A reveal basis for substrate specificity. *Nature* **448**, 87-91.
**Nilsson, M. E., Vandenput, L., Tivesten, A., Norlén, A.-K., Lagerquist, M. K., Windahl, S. H., Börjesson, A. E., Farman, H. H., Poutanen, M., Benrick, A. et al.** (2015). Measurement of a comprehensive sex steroid profile in rodent serum by high-sensitive gas chromatography-tandem mass spectrometry. *Endocrinology* **156**, 2492-2502.
**Ormandy, C. J., Camus, A., Barra, J., Damotte, D., Lucas, B., Buteau, H., Edery, M., Brousse, N., Babinet, C., Binart, N. et al.** (1997). Null mutation of the prolactin receptor gene produces multiple reproductive defects in the mouse. *Genes Dev.* **11**, 167-178.
**Patani, N., Jiang, W. G., Newbold, R. F. and Mokbel, K.** (2011). Histone-modifier gene expression profiles are associated with pathological and clinical outcomes in human breast cancer. *Anticancer Res.* **31**, 4115-4125.
**Pedersen, M. T., Agger, K., Laugesen, A., Johansen, J. V., Cloos, P. A. C., Christensen, J. and Helin, K.** (2014). The demethylase JMJD2C localizes to H3K4me3-positive transcription start sites and is dispensable for embryonic development. *Mol. Cell. Biol.* **34**, 1031-1045.
**Pedersen, M. T., Kooistra, S. M., Radzisheuskaya, A., Laugesen, A., Johansen, J. V., Hayward, D. G., Nilsson, J., Agger, K. and Helin, K.** (2016). Continual removal of H3K9 promoter methylation by Jmjd2 demethylases is vital for ESC self-renewal and early development. *EMBO J.* **35**, 1550-1564.
**Richter, K. S.** (2008). The importance of growth factors for preimplantation embryo development and *in-vitro* culture. *Curr. Opin. Obstet. Gynecol.* **20**, 292-304.
**Robertson, S. A., Roberts, C. T., Farr, K. L., Dunn, A. R. and Seamark, R. F.** (1999). Fertility impairment in granulocyte-macrophage colony-stimulating factor-deficient mice. *Biol. Reprod.* **60**, 251-261.
**Robertson, S. A., Mau, V. J., Young, I. G. and Matthaei, K. I.** (2000a). Uterine eosinophils and reproductive performance in interleukin 5-deficient mice. *J. Reprod. Fertil.* **120**, 423-432.
**Robertson, S. A., O'connell, A. C., Hudson, S. N. and Seamark, R. F.** (2000b). Granulocyte-macrophage colony-stimulating factor (GM-CSF) targets myeloid leukocytes in the uterus during the post-mating inflammatory response in mice. *J. Reprod. Immunol.* **46**, 131-154.
**Robertson, S. A., Sjöblom, C., Jasper, M. J., Norman, R. J. and Seamark, R. F.** (2001). Granulocyte-macrophage colony-stimulating factor promotes glucose transport and blastomere viability in murine preimplantation embryos. *Biol. Reprod.* **64**, 1206-1215.
**Sanford, T. R., De, M. and Wood, G. W.** (1992). Expression of colony-stimulating factors and inflammatory cytokines in the uterus of CD1 mice during days 1 to 3 of pregnancy. *J. Reprod. Fertil.* **94**, 213-220.
**Schatz, O., Golenser, E. and Ben-Arie, N.** (2005). Clearing and photography of whole mount X-gal stained mouse embryos. *BioTechniques* **39**, 650, 652, 654 passim.
**Sferruzzi-Perri, A. N., Macpherson, A. M., Roberts, C. T. and Robertson, S. A.** (2009). Csf2 null mutation alters placental gene expression and trophoblast glycogen cell and giant cell abundance in mice. *Biol. Reprod.* **81**, 207-221.

Development (2017) 144, 3264-3277 doi:10.1242/dev.155473

**Shin, S. and Janknecht, R.** (2007). Activation of androgen receptor by histone demethylases JMJD2A and JMJD2D. *Biochem. Biophys. Res. Commun.* **359**, 742-746.

**Slee, R. B., Steiner, C. M., Herbert, B.-S., Vance, G. H., Hickey, R. J., Schwarz, T., Christan, S., Radovich, M., Schneider, B. P., Schindelhauer, D. et al.** (2012). Cancer-associated alteration of pericentromeric heterochromatin may contribute to chromosome instability. *Oncogene* **31**, 3244-3253.

**Suzuki-Anekoji, M., Suzuki, A., Wu, S.-W., Angata, K., Murai, K. K., Sugihara, K., Akama, T. O., Khoo, K.-H., Nakayama, J., Fukuda, M. N. et al.** (2013). In vivo regulation of steroid hormones by the Chst10 sulfotransferase in mouse. *J. Biol. Chem.* **288**, 5007-5016.

**Van Casteren, J. I. J., Schoonen, W. G. and Kloosterboer, H. J.** (2000). Development of time-resolved immunofluorometric assays for rat follicle-stimulating hormone and luteinizing hormone and application on sera of cycling rats. *Biol. Reprod.* **62**, 886-894.

**Vaquerizas, J. M. and Torres-Padilla, M.-E.** (2016). Developmental biology: panoramic views of the early epigenome. *Nature* **537**, 494-496.

**Veselovska, L., Smallwood, S. A., Saadeh, H., Stewart, K. R., Krueger, F., Maupetit-Méhouas, S., Arnaud, P., Tomizawa, S., Andrews, S. and Kelsey, G.** (2015). Deep sequencing and de novo assembly of the mouse oocyte transcriptome define the contribution of transcription to the DNA methylation landscape. *Genome Biol.* **16**, 209.

**Whetstine, J. R., Nottke, A., Lan, F., Huarte, M., Smolikov, S., Chen, Z., Spooner, E., Li, E., Zhang, G., Colaiacovo, M. et al.** (2006). Reversal of histone lysine trimethylation by the JMJD2 family of histone demethylases. *Cell* **125**, 467-481.

**Whitten, W. K.** (1956). Modification of the oestrous cycle of the mouse by external stimuli associated with the male. *J. Endocrinol.* **13**, 399-404.

**Zhao, B., Zhang, W.-D., Duan, Y.-L., Lu, Y.-Q., Cun, Y.-X., Li, C.-H., Guo, K., Nie, W.-H., Li, L., Zhang, R. et al.** (2015). Filia is an ESC-specific regulator of DNA damage response and safeguards genomic stability. *Cell Stem Cell* **16**, 684-698.

**Zheng, P. and Dean, J.** (2009). Role of Filia, a maternal effect gene, in maintaining euploidy during cleavage-stage mouse embryogenesis. *Proc. Natl. Acad. Sci. USA* **106**, 7473-7478.